

Stabilization of broad-area VCSEL radiation by additional external optical beam

© E.A. Yarunova,^{1,2} A.A. Krents,^{1,2} N.E. Molevich^{1,2}

¹ Lebedev Physical Institute, Samara Branch, Russian Academy of Sciences,
443011 Samara, Russia

² Samara National Research University,
443086 Samara, Russia

e-mail: elisabetayarunova@yandex.ru

Received January 21, 2024

Revised January 21, 2024

Accepted January 21, 2024

In this paper, the dynamics of a broad-area semiconductor surface-emitting laser with a vertical resonator (VCSEL) is theoretically investigated. The freely generating laser is subject to modulation instability leading to radiation filamentation. A method of injecting external optical radiation to stabilize the dynamics of such a device is proposed. It is shown that a beam of external optical radiation of weak amplitude suppresses both the modulation instability developing in a broad-area VCSEL and the boundaries-induced filamentary dynamics. In addition, varying the beam width of the external optical radiation allows us to obtain various stationary spatial structures (rings and hexagons). The threshold values of the amplitude of external optical radiation necessary for stabilization depending on the beam width of external radiation and the curvature of the pump current profile are determined.

Keywords: VCSEL, modulation instability, optical injection, laser stabilization.

DOI: 10.21883/0000000000

Introduction

Semiconductor laser diodes with a traditional strip design have a broad range of practical applications. However, a considerable number of disadvantages of such devices stimulated the search for alternative designs of laser diodes, which include semiconductor lasers with a vertical cavity surface emitting laser (VCSEL). The group manufacturing technology and the ability to test devices directly on the manufactured board can be defined as the main features of VCSEL. At the moment, such devices are in high demand for solving various practical tasks. In particular, VCSEL are used in high-speed fiber-optic information transmission and processing systems, sensors and sensors of various types, and high-performance computer systems. At the same time, due to their small size, the output power may not be sufficient for efficient use. It is usually suggested to increase the transverse aperture of the device for solving this problem. But the implementation of such an approach, in turn, results in a significant deterioration of the quality of the beam due to the involvement of a large number of spatially transverse modes [1–3].

Broad-area lasers, in turn, can be divided into dynamic classes based on the characteristic values of the rates of relaxation processes (classes A, B, C, D) [4]. The lasers of the dynamic class B are the most common and sought-for in numerous applications. It is characteristic of this class that the relaxation rate of polarization is much higher than the relaxation rates of inversion and field. This particular class of lasers will be considered in this study. As previously

mentioned, the interaction of a large number of transverse modes results in the degradation of the quality of radiation, which is attributable to the development of various space-time instabilities. Semiconductor broad-area lasers of the class B are known to be characterized by the development of wave instability, which results in the filamentation of radiation [5–7]. Moreover, the Faraday instability may develop in class B lasers in case of a temporary modulation of the pump current, which may result in irregular dynamics, or to the formation of spatiotemporal patterns [8,9]. Broad-area vertical-cavity surface-emitting lasers (VCSEL) of class B are characterized by the modulation instability [10–13]. However, the same type of instability can also occur in class A lasers. Modulation instability is also the cause of highly irregular dynamics in the system, and can form stationary spatial structures: stripes and hexagons [14–17].

Effective approaches to the suppression of irregular space-time dynamics are needed for a wide practical use of VCSEL of class B. Quite a few different methods of laser beam stabilization have been proposed to date. A large number of studies address the methods based on spatial modulation of the pump current, refractive index and joint modulation of these two parameters [13,18–22]. It was also proposed to use spatiotemporal modulation of the pump current profile [10,11], but this stabilization method works most effectively in class A lasers, whereas it is effective only in a narrow range of modulation parameters in class lasers B. Another alternative approach was proposed in Ref. [23] based on the use of specially designed intracavity photonic crystals that modulate the refractive index in both the

longitudinal and transverse directions. At the same time, a significant improvement in the spatial quality of the output beam was obtained due to spatial filtration of radiation. Recently, it was proposed to change the geometry of the resonator [24], in particular its curvature [25,26] to improve the quality of laser radiation.

Circuits with feedback and additional external optical radiation is another direction of stabilization methods. Semiconductor lasers with optical injection have been studied quite widely, not only because of their numerous applications, but also because of the rich variety of their dynamic behavior. The continuous external optical radiation can act as a control input parameter and result in the formation of optical solitons [15,27–29]. The external optical radiation was also shown to be able to stabilize the dynamics of the laser [9,30–33]. There is a known effect of „frequency locking“, which allows locking the master laser with the slave in phase and frequency, which can improve the device characteristics with respect to frequency chirp and reduce noise [34–37]. It was proposed to use radiation filtering using the Fourier transform in feedback system in for improving the quality of radiation [38].

Moreover, the external additional radiation allows obtaining a spatially homogeneous beam. The external optical radiation of low amplitude was shown to suppress the radiation filamentation in semiconductor broad-area class B lasers caused by both wave instability and Faraday instability associated with time modulation of pumping [7,9,31].

It is impossible to completely match the frequency of the generated radiation with the external one in the optical injection experiments, but it was shown that the presence of a small frequency detuning does not destroy the stabilization effect [32,33]. The stabilization effect was achieved by suppressing relaxation oscillations characteristic of class B lasers.

The shape of the boundaries of the pumping region will affect the dynamics of the optical field in real broad-area lasers. A high sensitivity to the boundaries of the pumping region was found in class B semiconductor lasers for a widely used profile of the type „top-hat“, which results in a filamentous dynamics induced by the boundaries [5]. It was shown that the realistic case of optical injection in the form of a Gauss beam does not lose efficiency in the model for a broad-area semiconductor laser of class B [31], suppressing both the development of wave instability and filamentation associated with the impact of boundaries.

The external optical injection method can also be very effective for broad-area VCSELs. The weak coherent injection was shown to suppress the modulation instability in broad-area VCSEL [14,39]. However, the impact of optical injection on the simultaneous suppression of modulation instability and instability induced by boundaries in broad-area VCSEL has not been studied before.

The primary purpose of this study is to show that the irregular dynamics of the optical field of the broad-area VCSEL, caused by modulation instability and instabilities at the boundaries of the pump current profile, is effectively

suppressed by an external optical injection beam of weak amplitude, which makes it possible to obtain a spatially homogeneous laser beam. The impact of the injection beam width on the value of the injection threshold amplitude is studied in this paper, and the impact of the curvature of the pump current profile on the efficiency of the method is also considered. Moreover, it will be shown that it is possible to switch between different transverse stationary field distributions by varying the beam width of the external optical injection.

This study is organized as follows. A mathematical model describing VCSEL with additional external optical radiation is provided in Sec. 1. The stabilizing effect of optical injection is shown in Sec. 2 and the graphical dependencies that allow choosing the most effective characteristics of the external optical radiation beam for stabilization are also provided. The possibility of forming various stationary intensity distributions (rings and hexagons) depending on the beam width of external optical radiation is demonstrated in Sec. 3. The results obtained in this paper are discussed in the final section.

1. A mathematical model of a broad-area surface-emitting laser with external optical radiation

The dynamics of a broad-area VCSEL emitting in one longitudinal mode can be described using a system of Maxwell-Bloch differential equations for dimensionless envelopes of an electric field E and population inversion N [10,11]:

$$\begin{cases} \frac{\partial E}{\partial t} = -[1 + i\theta + 2C(i\alpha - 1)(N - 1)]E + i\Delta_{\perp}E + E_{inj}, \\ \frac{\partial N}{\partial t} = -\gamma[N - I + |E|^2(N - 1)] + \gamma d\Delta_{\perp}N. \end{cases} \quad (1)$$

Here Δ_{\perp} is a two-dimensional transverse Laplacian describing the diffraction and diffusion of carriers in the transverse direction. The carriers in the active region are generated by the pumping current I . The time t is normalized for the lifetime of the photon in the resonator $\tau_p = 11.7$ ns. Let L be the length of the cavity of the resonator, then the spatial coordinates (x, y) are normalized to $\sqrt{a} = \sqrt{L\lambda_0/2\pi T} = 4.39 \mu\text{m}$, where λ_0 is the central wavelength, and T is the transmission coefficient of the mirrors. The diffusion coefficient is determined by $d = l_D^2/a$, where $l_D = 1 \mu\text{m}$ is the characteristic diffusion length. $\theta = \omega\tau_p$ is frequency detuning of the resonator. Let's introduce a dynamic constant $\gamma = \tau_p/\tau_n$, where τ_n is the relaxation rate of population inversion. The envelopes were normalized as follows: $E = \sqrt{\frac{\epsilon n c \tau_n A}{\hbar \omega}} \tilde{E}$, $N = \frac{\tilde{N}}{N_0}$, $I = \frac{\tilde{I} \tau_n}{e V_a N_0}$, \tilde{E} , \tilde{N} , \tilde{I} are dimensional variables; V_a is volume of the active medium, N_0 is density of media at which the active medium becomes transparent, A is the gain factor. The value $C = \frac{ALN_0}{2T}$ is called the bistability parameter. The table shows the values of typical dimensionless physical

Basic physical parameters

Physical parameters of VCSEL, used for numerical calculations	
Mathematical Parameter Model	Value parameter
Diffusion parameter, d	0.052
Henry factor, α	1.5
Frequency detuning, θ	-1.5
Dynamic constant, γ	0.1
Bistability parameter, C	0.6

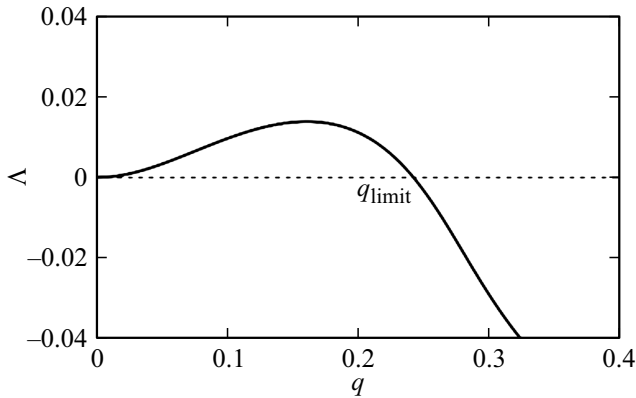


Figure 1. Dependence of the value of the real root Λ on the wave vector q of transverse modes (dispersion curve).

parameters of the system (1) [10,11], for which calculations were performed in this paper.

The study of the stability of a homogeneous stationary solution of a system of equations with respect to infinitesimal space-time perturbations is an universal method for studying possible dynamic processes in lasers. The homogeneous stationary solution of the system(1) has the following form in the absence of external optical radiation

$$N_0 = 1 + 1/2C, \quad E_0 = \sqrt{\frac{I - N_0}{N_0 - 1}}, \quad \theta = -\alpha. \quad (2)$$

The system of equations (1) was linearized earlier in Ref. [14] near the solution (2) and a cubic dispersion equation was obtained with respect to perturbations of the form $\exp(i(q_x x + q_y y) + \lambda t)$. The coefficients of this equation depend on q^2 , stationary values N_0 , $|E_0|^2$ and are given in Ref. [14,39]. The dependence of the value of the real root Λ of the obtained cubic dispersion equation on the wave vector q of the transverse modes (i.e., the dispersion curve) is shown Fig. 1 for the parameters from the table. There is a range of wave numbers $0 < q < q_{\text{limit}}$ for which the real root is positive, which indicates the modulation instability of the spatially transverse modes.

The wave transverse instabilities are characterized by the remaining pair of complex conjugate roots of the cubic dispersion equation. In this case, the real parts of the

complex conjugate roots for the system parameters from the table over the entire space of wave numbers are negative. This means that the spatially homogeneous generation mode (2) in this system is exposed only to one type of instability — modulation instability.

But such a conclusion, about the importance of the impact of only modulation instability on the dynamics of the laser field, is valid if the impact of the boundaries of the pumping region is not taken into account. A high sensitivity to the boundaries of the pumping region was found in Ref. [5] for class B laser, which can result in the filamentation induced namely by the boundaries in the absence of sufficient smoothing of the pumping profile. Therefore, the shape of the pump profile is usually close to uniform in the central part in broad-area laser with a relatively slow (smoothed) decrease towards the edges of the aperture.

We will use a pump current profile that meets these criteria to simulate the dynamics of VCSEL. In particular, they are well matched by a super-Gaussian profile, which has the following form

$$I = I_0 \exp(-0.5((x^2 + y^2)/w_0^2)^n), \quad (3)$$

for which we choose the amplitude of the pumping current $I_0 = 1.85$, w_0 determines the distance at which the pumping current decreases by $\sqrt[n]{e}$ times, and the value n is the rate (sharpness) of the profile amplitude decay at the edges of the aperture compared to the value on the axis.

The implicit Crank-Nicholson scheme which is certainly stable was used for the numerical solution of a system of equations (1). A spatially homogeneous laser generation mode was chosen as the initial conditions (2) with the addition of low amplitude noise. The irregular dynamics develops both in time and in the beam cross-section as a result of the presence of modulation instability in the system and taking into account instabilities caused by the boundaries of the pumping region (Fig. 2). Obviously, such dynamics of the optical field greatly limits the use of such lasers. Sec. 2 shows how the external optical

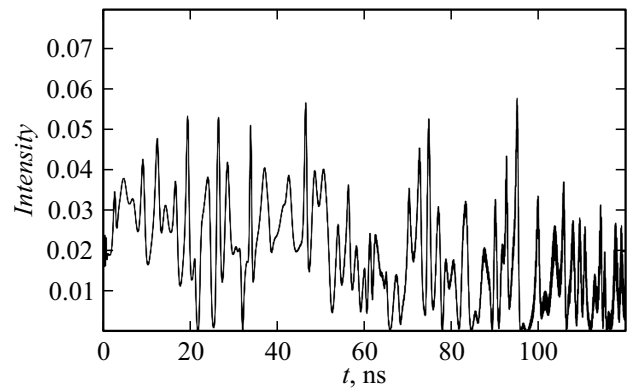


Figure 2. Dependence of the generation intensity on time for the parameters from the table and the pump profile in the form (3) with $I_0 = 1.85$, width $w_0 = 350 \mu\text{m}$ and $n = 10$.

injection method can improve the optical quality of broad-area VCSELs.

2. Stabilizing effect of optical injection

The external optical injection can effectively suppress modulation instability and stabilize the dynamics of VCSEL as shown in detail in Ref. [14,39]. Let’s briefly look at why this is happening. The addition of external optical radiation of amplitude E_{inj0} , resonant to the laser generation frequency, strongly changes the homogeneous stationary solution for the field (2), which is now described by the implicit expression (4):

$$|E_{inj0}|^2 = |E_0|^2 \left[\left(-\alpha + 2C\alpha \left(\frac{I + |E_0|^2}{|E_0|^2 + 1} - 1 \right) \right)^2 + \left(1 - 2C \left(\frac{I + |E_0|^2}{|E_0|^2 + 1} - 1 \right) \right)^2 \right]. \quad (4)$$

The stationary value N_0 is still determined by the expression (2).

Implicit expression (4) connects the values of the amplitude of the external optical radiation and the corresponding new stationary values. A nontrivial stationary solution E_0 of the form (2) is obtained from (4) with $E_{inj0} = 0$. It is equal to $E_0 \approx 0.14$ for parameters from the table.

The study of the roots of the cubic dispersion equation obtained by linearization near the stationary state (4) allows constructing a bifurcation diagram (Fig. 3) on the plane of transverse wave vectors q and stationary values E_0 (4), determined depending on injection amplitudes. An increase of the amplitude of the external optical injection changes the homogeneous stationary value E_0 and reduces the region of unstable wave numbers at which the real root Λ of the dispersion equation is positive. The critical value of the

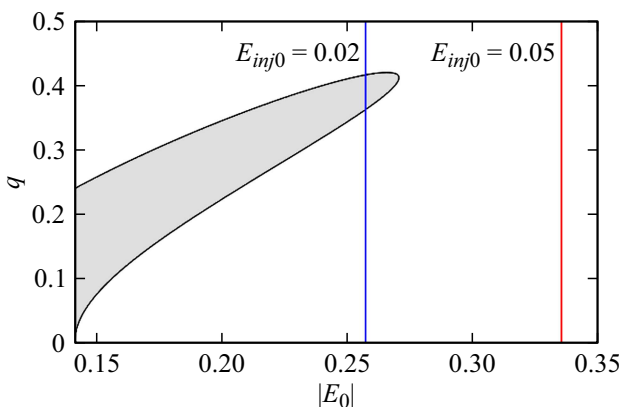


Figure 3. Bifurcation diagram for wave numbers q and the modulus of stationary values of the amplitude of the optical field E_0 . The area of modulation instability is shaded in gray. The blue line highlights a range of unstable wavenumbers with an injection amplitude of 0.02. The absence of intersections of the red line (for the injection amplitude 0.05) with the modulation instability region indicates stabilization of the radiation.

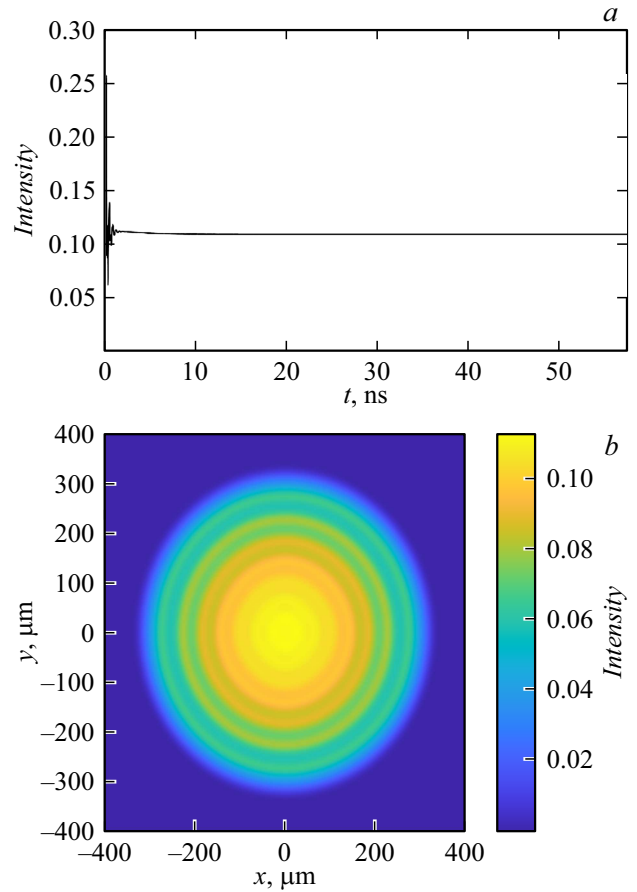


Figure 4. Intensity distribution for the parameters from the table and the pump profile in the form (3) with $I_0 = 1.85$, width $w_0 = 350\mu\text{m}$ and $n = 10$ and the shape of the external optical injection beam (5) with amplitude $E_{inj0} = 0.05$ and width $w = 263\mu\text{m}$ (a) time dependence (b) transverse intensity distribution in time moment 40 ns.

injection amplitude will be equal to $E_{inj0} = 0.03$ for the considered parameters. The region of unstable q does not exist with $E_{inj0} > 0.03$, i.e. the laser generation is stabilized.

The effective stabilization described above was achieved under the assumption of flat pump profiles and optical injection. For a practical assessment of the effectiveness of the optical injection method, it is desirable to take into account both the current pumping profile of the laser and the impact of the shape of the external radiation beam. For this purpose the dynamics of a laser described by a system of equations (1), parameters from the table, with a pump profile (3) and an optical injection beam of the form was numerically calculated in this paper

$$E_{inj} = E_{inj0} \exp(-(x^2 + y^2)/w^2), \quad (5)$$

where E_{inj0} — radiation amplitude, w — beam width.

The numerical solution of a system of differential equations (1) taking into account the shape of the external optical radiation beam and the pump current profile showed that instabilities are still effectively suppressed (Fig. 4, a) and an unfiltered output beam is acquired. Taking into account

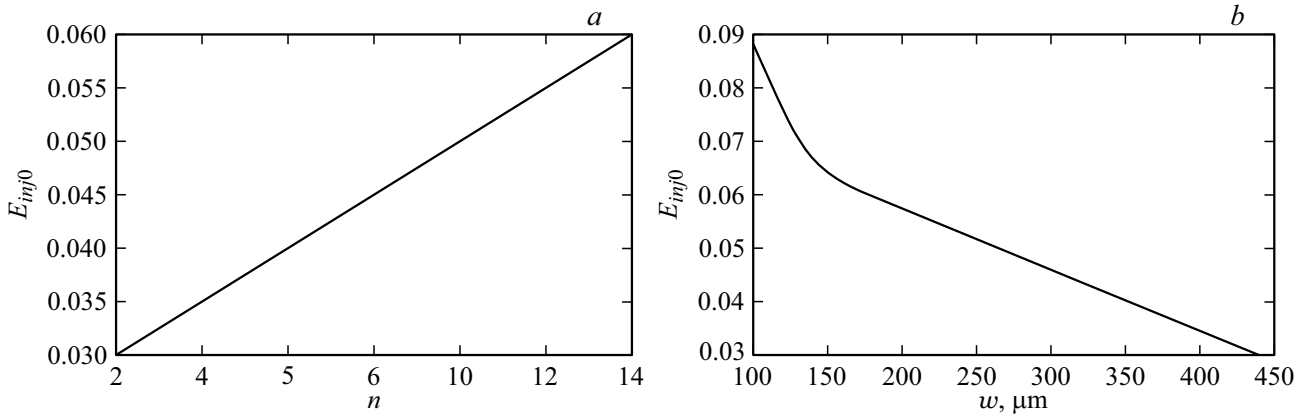


Figure 5. *a* is the dependence of the threshold amplitude E_{inj0} of injection (beam width $w = 263 \mu\text{m}$) on the degree of curvature n of the pump profile, which is set as (3) with $I_0 = 1.85$ and width $w_0 = 350 \mu\text{m}$; *b* is the dependence of threshold amplitude E_{inj0} on beam width w external radiation for the pump current profile (3) with $I_0 = 1.85$, $n = 10$, and $w_0 = 350 \mu\text{m}$.

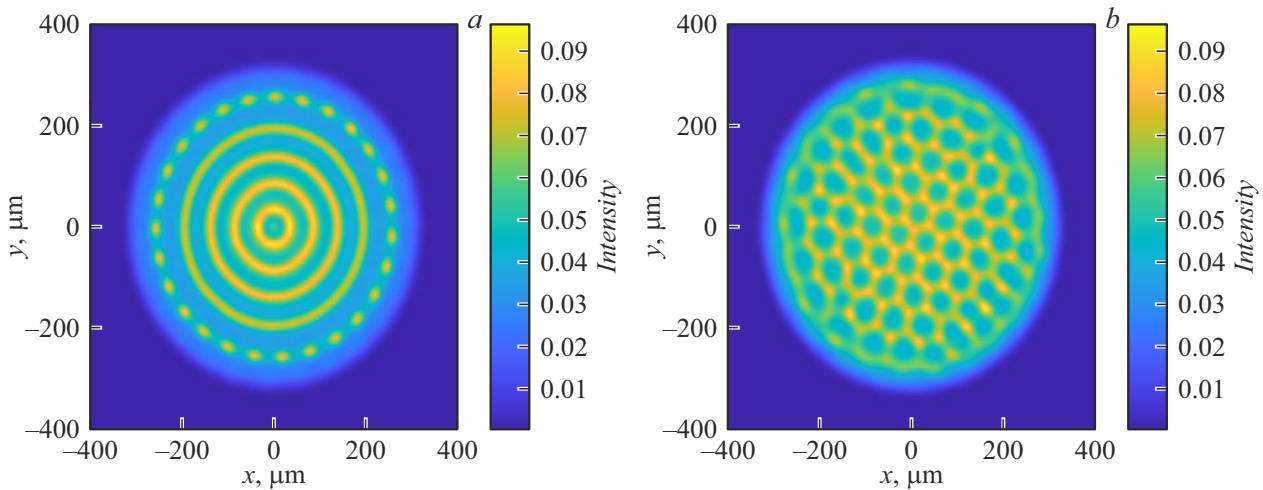


Figure 6. *a* — stationary distribution of the intensity in the form of 5 rings in case of presence of an external optical radiation in the form of a Gaussian beam with an amplitude of $E_{inj0} = 0.02$ and width of $w = 263 \mu\text{m}$; *b* — stationary distribution of the intensity in the form of hexagons with the presence of an external optical radiation in the form of a Gaussian beam with an amplitude of $E_{inj0} = 0.02$ and width of $w = 439 \mu\text{m}$.

realistic contact forms of the pump current and the external radiation beam does not destroy the stabilization effect, but a time-stable intensity distribution occurs, which is close to homogeneous distribution in cross section with a weak modulation (Fig. 4, *b*).

At the same time, our calculations show that the threshold value of the injection amplitude at which stabilization is observed significantly depends on the shape of the pump profile. In particular, the injection threshold value decreases in case of smoothing the sharp edges of the pump profile (decrease of n) which indicates a decrease of sensitivity to edge effects. The resulting dependence is shown in Fig. 5, *a*. The beam has a shape with a flatter top and sharp edges in case of large values of n . The amplitude threshold of optical injection was found to generally decrease by about 2 times with a decrease of the degree of n . The dependence

of the threshold injection amplitude on the width of the injection beam is also determined (Fig. 5, *b*). As expected for boundary-induced instability, the threshold of stabilizing injection strongly depends on the amplitude of the injection beam near the pump edges. The threshold amplitude of the external radiation rapidly decreases with an increase of the width of the injection beam and tends to the limit value $E_{inj0} = 0.03$, corresponding to the flat injection front.

3. Formation of stationary spatial structures in a broad-area laser with external optical injection

Modulation instability can result not only in spatially irregular dynamics, but also in the formation of stationary spatial structures. Ref. [14] showed that it is possible

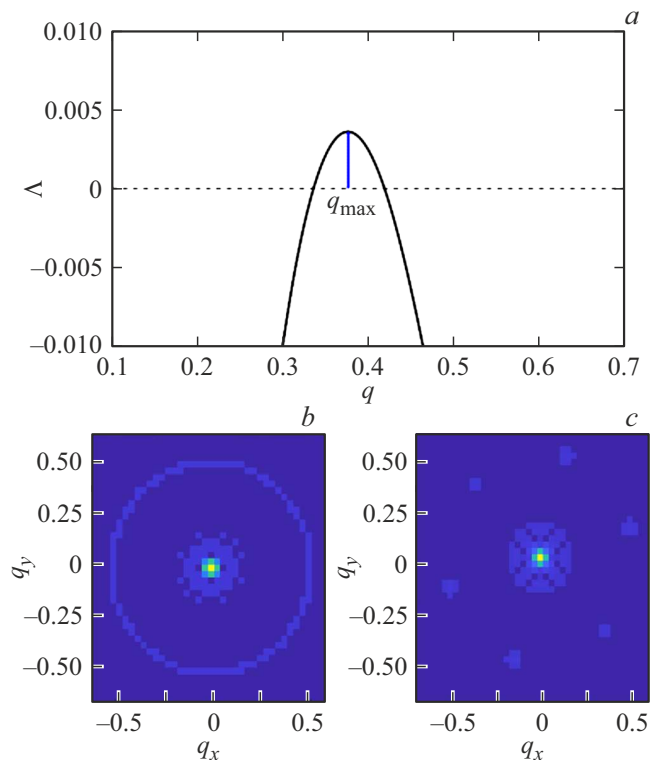


Figure 7. *a* — dispersion curve demonstrating the maximum increment of increase for the injection amplitude $E_{inj0} = 0.02$; *b* — spatial spectrum for the case of 5 rings; *c* — spatial spectrum for hexagons.

to form stationary optical fields in the form of stripes and hexagons in the broad-area VCSEL system by correct selection of the amplitude of the external optical injection, which is represented by a flat front. Earlier, it was shown in Fig. 3 that external optical radiation with an amplitude of $E_{inj0} = 0.02$ shifts the homogeneous stationary solution E_0 along the bifurcation diagram (blue line), as a result of which the region of unstable wavenumbers q is significantly reduced, this favours the formation of regular patterns instead of chaotic filamentation of the optical field.

The results of numerical modeling showed that taking into account the shapes of the pump current profile (3) and the external optical injection beam (5) does not prevent the formation of stationary regular spatial structures. Rings were obtained instead of stripes in the considered geometry. Moreover, it was found using numerical modeling for the first time that it is possible to switch between rings and hexagons by changing the beam width of external optical radiation. For example, it was shown that an intensity distribution in the form of five rings is formed for an external optical injection beam with an amplitude of $E_{inj0} = 0.02$ and a width of $w = 263 \mu\text{m}$ as shown in Fig. 6, *a*. By increasing the beam width of the external optical injection to $w = 439 \mu\text{m}$, it is possible to obtain a stationary distribution in the form of hexagons, as shown in Fig. 6, *b*. The

mechanisms of the emergence of such structures and the switching between them deserve further study.

It is possible to state that the spatial size of the obtained structures correlates with the results of the linear analysis of a stable dynamic system (1). In fact, a disperse curve for the case with injection $E_{inj0} = 0.02$ is plotted on Fig. 7, *a*. Wave number $q_{\text{max}} \approx 0.38$ for which the value of the valid root is maximum is marked on this curve. The spatial mode with the largest eigenvalue results in its strengthening by suppressing all other growing modes according to the „winner-takes-all“ circuit. A spatial spectrum of the far field was obtained for the case of five rings using the inverse Fourier transform, (Fig. 7, *b*), on which, in addition to the central peak of the finite width (due to the finite width of the pump profile), a secondary maximum in the form of a ring with a radius of 0.5 is clearly visible. The radius of the ring is in satisfactory agreement (within 20%) with linear analysis results. The error is explained by the contribution of nonlinear effects of harmonic interaction in the formation of such essentially nonlinear stationary spatial structures. The spatial spectrum for hexagons (Fig. 7, *c*) is also in satisfactory agreement with linear analysis.

Therefore, stationary spatial structures of various shapes can be obtained by varying the parameters of external optical radiation. Similar spatial intensity distributions can be used in many applications, including optical memory. The study of the processes of formation of such structures makes it possible to control the spatiotemporal intensity profile and generate optical radiation with the required output characteristics.

Conclusion

In this work, it is theoretically demonstrated that external optical radiation can effectively stabilize the dynamics of a broad-area semiconductor laser with a vertical resonator of class B. At the same time, non-planar profiles of the pump current and the injection beam were taken into account. Based on the Maxwell-Bloch equation system, the efficiency of optical injection was studied to suppress both modulation instability and instabilities induced by the boundaries of the pumping current in a class B laser. The proposed method of external optical injection makes it possible to change the spatiotemporal distribution of the intensity of the generated radiation from highly irregular to spatially homogeneous with weak modulation in the beam cross section.

Moreover, the external optical radiation makes it possible to obtain stationary spatial optical structures of various shapes. The type of stationary spatial structures can be controlled by changing the amplitude and width of the beam of external optical radiation.

The revealed stabilization effect turns out to be quite sensitive to the shape of the pump current profile. The efficiency of the injected radiation increases as the edges of this profile are smoothed. The dependences of the threshold amplitude of the external optical radiation on the degree of

curvature of the profile and the beam width of the external optical injection are obtained.

Therefore, the work demonstrates that external radiation effectively suppresses instabilities, which makes it possible to obtain an unfilamented output beam regardless of the impact of boundaries.

Funding

The study has been performed under the state assignments of Lebedev Physical Institute and Samara University, supported by the Ministry of Science and Higher Education of the Russian Federation (project № FSSS-2023-0009).

Conflict of interest

The authors declare that they have no conflict of interest.

References

- [1] P.K. Jakobsen, J.V. Moloney, A.C. Newell, R. Indik. *Phys. Rev. A.*, **45** (11), 8129 (1992). DOI: 10.1103/physreva.45.8129
- [2] A.P. Zaikin, N.E. Molevich. *Quant. Electron.*, **34** (8), 731 (2004). DOI: 10.1070/QE2004v034n08ABEH002663
- [3] D. Amroun, M. Brunel, C. Letellier, H. Leblond, F. Sanchez. *Phys. D*, **203**, 185 (2005). DOI: 10.1016/j.physd.2005.03.015
- [4] Ya.I. Khanin, *Osnovy dinamiki lazerov* (M., Nauka, 1999) (in Russian).
- [5] A.V. Pakhomov, N.E. Molevich, A.A. Krents, D.A. Anchikov. *Opt. Commun.*, **372**, 14 (2016).
- [6] D.A. Anchikov, A.A. Krents, N.E. Molevich. *Comp. Opt.*, **41** (3), 363 (2017). DOI: 10.18287/2412-6179-2017-41-3-363-368
- [7] D.A. Anchikov, A.A. Krents, N.E. Molevich. *Comp. Opt.*, **40** (1), 31 (2016). DOI: 10.18287/2412-6179-2016-40-1-31-35
- [8] A.A. Krents, N.E. Molevich, D.A. Anchikov. *J. Opt. Soc. Am. B*, **34** (8), 1733 (2017). DOI: 10.1364/JOSAB.34.001733
- [9] E.A. Yarunova, A.A. Krents, N.E. Molevich. *Radiophys. Quant. Electron.*, **64** (4), 290 (2021). DOI: 10.1007/s11141-021-10131-6
- [10] W.W. Ahmed, S. Kumar, R. Herrero, M. Botey, M. Radziunas, K. Staliunas. *Phys. Rev. A*, **92** (4), 043829 (2015). DOI: 10.1103/PhysRevA.92.043829
- [11] W.W. Ahmed, S. Kumar, R. Herrero, M. Botey, M. Radziunas, K. Staliunas. *Proc SPIE Nonlinear Optics Applications IV*, **9894** (2016). DOI: 10.1117/12.2227801
- [12] K. Panajotov, M. Tlidi. *Eur. Phys. J. D*, **59** (1), 67 (2010). DOI: 10.1140/epjd/e2010-00111-y
- [13] S. Kumar, R. Herrero, M. Botey, K. Staliunas. *Opt. Lett.*, **39** (19), 5598 (2014). DOI: 10.1364/ol.39.005598
- [14] E.A. Yarunova, A.A. Krents, N.E. Molevich. *Opt. Lett.*, **48** (15), 4021 (2023). DOI: 10.1364/OL.495570
- [15] L. Spinelli, G. Tissoni, M. Brambilla, F. Prati, L.A. Lugiato. *Phys. Rev. A*, **58** (3), 2542 (1998). DOI: 10.1103/physreva.58.2542
- [16] G. Tissoni, L. Spinelli, M. Brambilla, T. Maggipinto, I.M. Perrini, L.A. Lugiato, *J. Opt. Soc. Am. B*, **16** (11), 2095 (1999). DOI: 10.1364/josab.16.002095
- [17] E.A. Yarunova, A.A. Krents, N.E. Molevich. *Opt. Memory*, **32** (Suppl 1), 46 (2023). DOI: 10.3103/S1060992X2305020X
- [18] R. Herrero, M. Botey, M. Radziunas, K. Staliunas. *Opt. Lett.*, **37** (24), 5253 (2012). DOI: 10.1364/ol.37.005253
- [19] M. Radziunas, R. Herrero, M. Botey, K. Staliunas. *J. Opt. Soc. Am. B*, **32** (5), 993 (2015). DOI: 10.1364/josab.32.000993
- [20] M. Radziunas, M. Botey, R. Herrero, K. Staliunas. *Appl. Phys. Lett.*, **103** (13), 2 (2013). DOI: 10.1063/1.4821251
- [21] W.W. Ahmed, S. Kumar, J. Medina, M. Botey, R. Herrero, K. Staliunas. *Opt. Lett.*, **43** (11), 2511 (2018). DOI: 10.1364/OL.43.002511
- [22] J. Medina Pardell, R. Herrero, M. Botey, K. Staliunas. *Phys. Rev. A*, **101** (3), 33833 (2020). DOI: 10.1103/physreva.101.033833
- [23] D. Gailevicius, V. Koliadenko, V. Purlys, M. Peckus, V. Taranencko, K. Staliunas. *Sci. Rep.*, **6** (1), 34173 (2016). DOI: 10.1038/srep34173
- [24] K. Kim, S. Bittner, Y. Jin, Y. Zeng, Q.J. Wang, H. Cao. *Opt. Lett.*, **48** (3), 574 (2023). DOI: 10.1364/OL.479901
- [25] K. Kim, S. Bittner, Y. Jin, Y. Zeng, S. Guazzotti, O. Hess, Q.J. Wang, H. Cao. *APL Photon.*, **7**, 056106 (2022). DOI: 10.1063/5.0087048
- [26] S. Bittner, K. Kim, Z. Yongquan, Q. Wang, H. Cao. *New J. Phys.*, **22** (8) 083002 (2020). DOI: 10.1088/1367-2630/ab9e33
- [27] L. Spinelli, G. Tissoni, M. Tarengi, M. Brambilla. *Eur. Phys. J. D*, **15**, 257 (2001). DOI: 10.1007/s100530170174
- [28] M. Brambilla, L.A. Lugiato, F. Prati, L. Spinelli, W.J. Firth. *Phys. Rev. Lett.*, **79**, 2040 (1997). DOI: 10.1103/physrevlett.79.2042
- [29] E.A. Yarunova, A.A. Krents, N.E. Molevich. *Uchenye zapiski fiz. fak. Moskovskogo un-ta*, **4**, 2341001 (2023) (in Russian).
- [30] S. Takimoto, T. Tachikawa, R. Shogenji, J. Ohtsubo. *IEEE Photon. Technol. Lett.*, **21** (15), 1051 (2009). DOI: 10.1109/LPT.2009.2022181
- [31] A.V. Pakhomov, R.M. Arkhipov, N.E. Molevich. *J. Opt. Soc. Am. B*, **34** (4), 756 (2017). DOI: 10.1364/josab.34.000756
- [32] E.A. Yarunova, A.A. Krents, N.E. Molevich, D.A. Anchikov. *Bull. Lebedev Phys. Inst.*, **46** (4), 130 (2019). DOI: 10.3103/S1068335619040067
- [33] E.A. Yarunova, A.A. Krents, N.E. Molevich, D.A. Anchikov. *Bull. Lebedev Phys. Inst.*, **48** (2), 35 (2021). DOI: 10.3103/S1068335621020081
- [34] C. Chang, S. Member, L. Chrostowski, S. Member. *IEEE J. Sel. Top. Quant. Electron.*, **9** (5), 1386 (2003). DOI: 10.1109/JSTQE.2003.819510
- [35] D. Parekh. *Optical Injection Locking of Vertical Cavity Surface-Emitting Lasers: Digital and Analog Applications* (UC Berkeley, 2012)
- [36] G. Oppo, H.G. Solari. *Nonlinear Dynamics in Optical Systems*, Technical Digest Series. LD342 (1990). DOI: 10.1364/NLDOS.1990.LD342
- [37] R. Ye, W. Wang, J. Zhu, X. Zeng, Y. Cai, Shixiang. *Proc. SPIE*, **12757**, DOI: 10.1117/12.2690199
- [38] G.K. Harkness, R. Martin, G. Oppo, W.J. Firth. *Europ. Quant. Electron. Conf.*, Tech. Digest Series, paper QTuF6 (1998). DOI: 10.1109/eqec.1998.714743
- [39] E.A. Yarunova, A.A. Krents, N.E. Molevich. *Comp. Opt.*, **47** (6), 920 (2023). DOI: 10.18287/2412-6179-CO-1288

Translated by A.Akhtyamov